Published by
NIGERIAN SOCIETY OF PHYSICAL SCIENCES
Available online @ https://journal.nsps.org.ng/index.php/jnsps

J. Nig. Soc. Phys. Sci. 6 (2024) 1934

Journal of the Nigerian Society of Physical Sciences

Effect of magnetic field on the onset of thermal convection in a Jeffery nanofluid layer saturated by a porous medium: free-free, rigid-rigid and rigid-free boundary conditions

Ajit Kumar[a], Pushap Lata Sharma[a,*], Praveen Lata[a], Deepak Bains[a], Pankaj Thakur[b]

[a]*Department of Mathematics & Statistics, Himachal Pradesh University, Summer Hill, Shimla, India*
[b]*Faculty of Science and Technology, ICFAI University, Baddi, Solan, India*

Abstract

The effect of the magnetic field on the onset of thermal convection in a porous layer saturated by Jeffrey nanofluid is studied. Three distinct boundary conditions are considered to be free-free, rigid-rigid and rigid-free boundaries. The model used for Jeffrey nanofluid includes the effect of Brownian motion and thermophoresis. The normal mode analysis as well as the Galerkin first approximation technique is used. The effects of the Rayleigh number of nanoparticles, Lewis number, modified diffusivity ratio, Jeffery parameter, porosity and Chandrasekhar number are investigated analytically and graphically. It is discovered that the Chandrasekhar number, Lewis number and modified diffusivity ratio have a stabilizing effect while the Jeffery parameter, nanoparticles Rayleigh number and porosity have a destabilizing effect. This study induces the effect of Chandrasekhar number and Jeffrey nanofluid. We have analyzed that Chandrasekhar number produces a stabilizing effect on the onset of convection i.e. it delays the onset of convection whereas the Jeffrey parameter which comes from Jeffrey nanofluid shows the destabilizing effect on the onset of convection i.e. it accelerates the onset of convection. The influence of a magnetic field on the commencement of nanofluid convection is significant in magnetohydrodynamic power generators, electrical equipment, petroleum reservoirs, nuclear reactors, biochemical engineering, chemical engineering and geophysics.

DOI:10.46481/jnsps.2024.1934

Keywords: Magnetic field; thermal convection; Jeffery nanofluid; normal mode technique

Article History :
Received: 15 December 2023
Received in revised form: 12 March 2024
Accepted for publication: 31 March 2024
Published: 21 April 2024

Communicated by: B. J. Falaye

1. Introduction

A nanofluid is a colloidal suspension consisting of nanoparticles (typically less than 100 nanometers in size) dispersed in a base fluid. Choi [1] is credited with coining the term "nanofluid". The application of nanofluid in porous materials across automotive, energy efficiency, nuclear reactor, transformer, medical (especially hyperthermia treatment) and various other industries has sparked increased attention among researchers. Several studies have demonstrated that certain nanofluid formulations can effectively eliminate cancerous cells while preserving the integrity of healthy organs.

Buongiorno's model refers to the theoretical framework proposed by Buongiorno [2] in his research, typically address-

*Corresponding author tel. no: +917018937046
Email addresses: ajitkoundal@gmail.com (Ajit Kumar), pl_maths@yahoo.in (Pushap Lata Sharma)

ing phenomena related to the behavior, dynamics or properties of nanofluids in various contexts, such as heat transfer, fluid flow thermal instability, particularly within porous media. Many researchers have examined the Buongiorno model of thermal instability of nanofluid in a porous medium and they have discovered applications for it in the molten cores of Earth, oil reservoirs, bile ducts, gall bladders with stones in blood veins, human lungs etc. Chandrasekhar [3] journeyed to gain a deeper understanding of thermal instability in Newtonian fluids. Nield and Kuznetsov [4] carved out a noteworthy path through the maze of porous media convection.

Meanwhile, researchers like Tzou [5, 6], Nield and Bejan [7] and Sheu [8] have broken new ground by deciphering the mystery of nanofluid convection using a range of theoretical models. Through their recent research, Rana *et al.* [9] and Sharma *et al.* [10, 11] have illuminated the intricate subject of thermal instabilities and explored the intriguing realm of non-Newtonian fluid.

Using the Brinkman model, Nield and Kuznetsov [12] examined a variety of boundary conditions, when examining heat convection in nanofluids inside porous media. In our research we have proposed Darcy model for porous media. Darcy simply proposed the relationship between rate of fluid flow and applied pressure gradient in his model. Numerous authors like Gautam *et al.* [13] and Sharma *et al.* [14–16] have utilized Darcy model in their investigations. The study of heat transmission in a fluid in a porous medium is crucial because it has numerous uses in industries like engineering (for chemical reactor construction), geothermal reservoirs, building insulation (for the production of fiberglass), etc. The buoyant force produced when internal heat production and vertical throughflow are combined is one of the main research interests in the onset of convective movement in a porous medium.

We have already covered a lot of ground in our extensive discussion of Newtonian nanofluid research. The bulk of industrial and biological nanofluids exhibit non-Newtonian rheological behaviour, making Newton's law of viscosity inadequate to adequately characterize their behaviour. These fluids are used in many different disciplines, such as chemistry, geophysics and biological sciences. Biological liquids such as blood and motor oil, as well as drilling muds, soap solutions, sauces, foams, paints and lubricants are examples of non-Newtonian nanofluids. The study of non-Newtonian nanofluids in porous media has not received much attention, different types of non-Newtonian nanofluids exist. The Jeffrey fluid model, recognized as the most valuable among these models, has garnered significant interest from various researchers, including Gautam *et al.* [13], Sharma *et al.* [14–16], Rana [17], Khan *et al.* [18], Pati *et al.* [19], Pati *et al.* [20], Ashraf *et al.* [21], Sharma *et al.* [22], Bains *et al.* [23] and Garg *et al.* [24–28].

Magnetic field is important when studying thermal instability of a fluid layer heated from below. Numerous domains, such as fluid machinery, mechanical engineering, geophysics, biomechanics, power plants and the automotive and petroleum sectors can be benefited from its applications. Bains and Sharma [29] and Sharma et al. [30] have investigated the problem, effects of magnetic field on thermal and thermosolutal convection in Jeffrey nanofluid with porous medium. Sharma *et al.* [31] has investigated several thermosolutal instability issues in a horizontal layer of porous material saturated by a nanofluid using computational and analytical methods. Recent work on magnetic field under the consideration of Jeffrey nanofluid, under different circumstances are conducted by many researchers like: Yadav [32–35] and Yadav *et al.* [36, 37]. Gupta *et al.* [38] investigated the megneto convection within the nanofluid layers.

The current work was prompted by the increasing number of applications of nanofluid, which include numerous industries such as the pharmaceutical and energy supply industries, as well as several medical fields such as cancer therapy. Our primary goal is to investigate magneto convection in a porous medium's Jeffery nanofluid, which has boundaries that are rigid-free, free-free and rigid-rigid. As far as we are aware, this paper has not yet been published.

2. Mathematical formulation

We have considered an infinite horizontal layer of Jeffery nanofluid of thickness d between the planes $z = 0$ and $z = d$ in the presence of consistent magnetic field $h = (0, 0, h)$. The nanofluid layer is heated from bottom layer and working upwards direction with gravity force $\mathbf{g} = g(0, 0, -g)$ (refer Figure 1), where the temperatue T and volumetric fraction φ of nanoparticles are kept constant at $z = 0$ and $z = d$, with $T_0 > T_1$ and $\varphi_0 > \varphi_1$.

2.1. Governing equations

Equation of continuity is given by:

$$\nabla \cdot \boldsymbol{q}_D = 0. \tag{1}$$

Equation of motion by Boussinesq [2] approximation is given by:

$$\begin{aligned} &\frac{\rho_f}{\varepsilon}\left(\frac{\partial \boldsymbol{q}_D}{\partial t} + \frac{1}{\varepsilon}\left(\boldsymbol{q}_D \cdot \nabla\right)\boldsymbol{q}_D\right) = -\nabla p - \frac{\mu}{k_1(1+\lambda_3)}\boldsymbol{q}_D \\ &+ \frac{\mu_e}{4\pi}\left(h \cdot \nabla\right)h + \left(\varphi\rho_p + (1-\varphi)\left\{\rho_0\left(1 - \alpha\left(T - T_1\right)\right)\right\}\right)\boldsymbol{g}, \end{aligned} \tag{2}$$

where λ_3 denotes Jeffery parameter, ρ_f denotes fluid density, ρ_p denotes fluid pressure, T denotes fluid temperature, μ denotes fluid viscosity and ϵ denotes porosity.

The Brownian diffusion coefficient D_B and the thermophoretic diffusion coefficient D_T are defined respectively, as:

$$D_B = \frac{k_B T}{3\pi\rho_f d_p}, \quad D_T = \frac{\rho_f 0.26 k_f}{\rho_f(2k_f + k_p)}\varphi.$$

The momentum-balance equation of nanoparticle is given by

$$\left[\frac{\partial}{\partial t} + \frac{q_D \cdot \nabla}{\epsilon}\right]\epsilon = D_B\nabla^2\varphi + \frac{D_T}{T_1}\nabla^2 T. \tag{3}$$

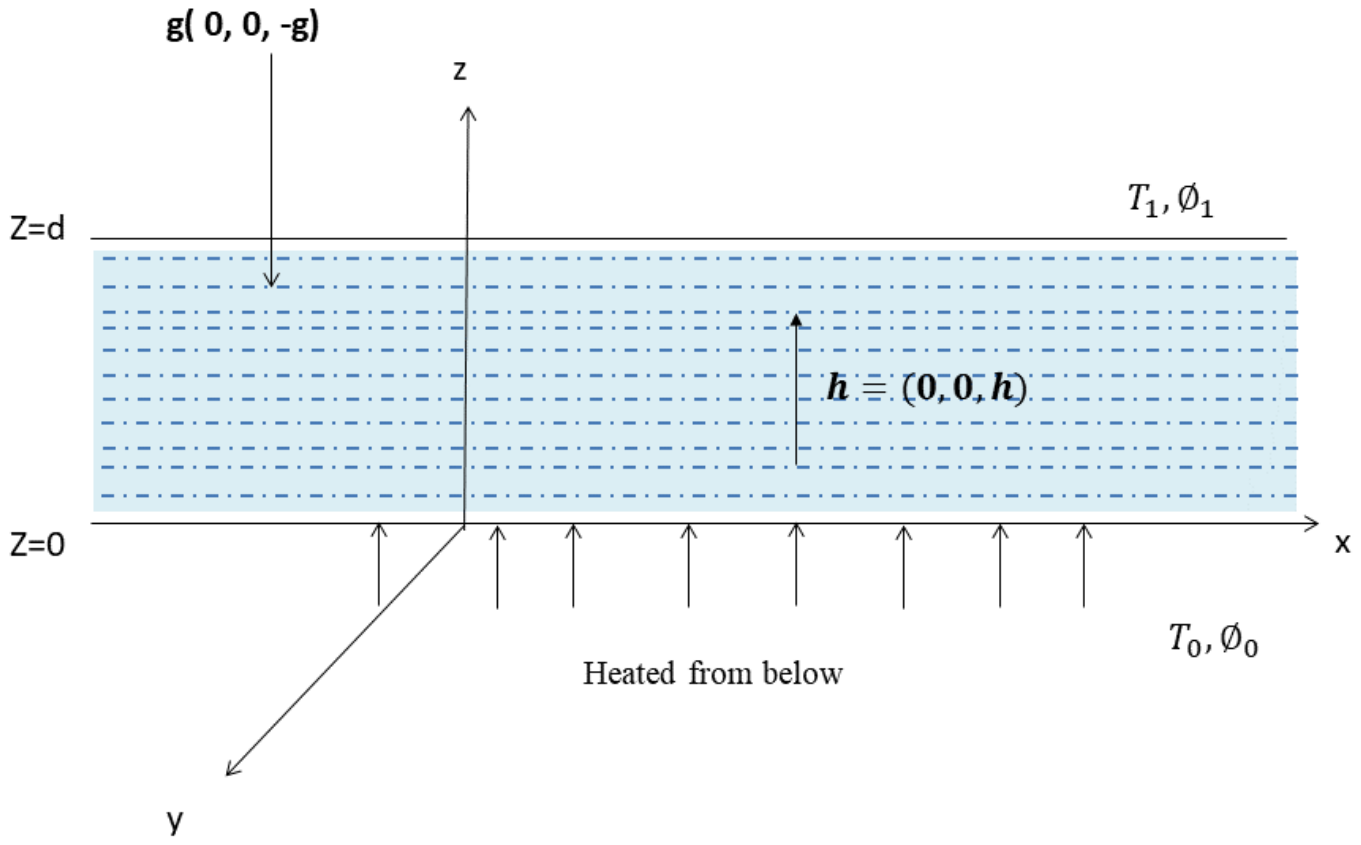

Figure 1. Physical configuration.

The energy-balance equation is given by [3, 10, 30]:

$$\frac{\partial T}{\partial t}(\rho c)_m + \boldsymbol{q}_D \cdot \nabla T (\rho c)_f = k_m \nabla^2 T + \left[D_B \nabla\varphi \cdot \nabla T + \frac{D_T}{T_1} \nabla T \cdot \nabla T \right] \varepsilon (\rho c)_p, \tag{4}$$

The Maxwell equation is given as

$$\frac{\partial h}{\partial t} + (\boldsymbol{q}_D.\nabla) h = (h.\nabla) \boldsymbol{q}_D + \eta \nabla^2 h, \tag{5}$$

$$\nabla.h = 0, \tag{6}$$

where η represents resistivity of the fluid. The boundary conditions are

$$\left.\begin{array}{llll} w = 0, & \varphi = \varphi_0 & T = T_0, & at \quad z = 0 \\ w = 0, & \varphi = \varphi_1 & T = T_1, & at \quad z = d \end{array}\right\}. \tag{7}$$

Omitting the dashes ($'$) for convenience. Eqs. (1) - (6) reduce to the non-dimensional form:

$$\nabla \cdot \boldsymbol{q}_D = 0, \tag{8}$$

$$\left(\frac{1}{v_a}\frac{\partial}{\partial t} + \frac{1}{1+\lambda_3}\right) w = -\lambda p - R_m \hat{e}_z + R_a T \hat{e}_z - R_n \varphi \hat{e}_z + Q \frac{Pr_1}{Pr_2} (h \cdot \nabla) h, \tag{9}$$

$$\frac{1}{\sigma}\frac{\partial \varphi}{\partial t} + \frac{1}{\varepsilon}\boldsymbol{q}_D \cdot \nabla\varphi = \frac{1}{L_n}\nabla^2\varphi + \frac{N_A}{L_n}\nabla^2 T, \tag{10}$$

$$\frac{\partial T}{\partial t} + \boldsymbol{q}_D \cdot \nabla T = \nabla^2 T + \frac{N_B}{L_n}\nabla\varphi \cdot \nabla T + \frac{N_A N_B}{L_n}\nabla T \cdot \nabla T, \tag{11}$$

$$\frac{\partial h}{\partial t} + \sigma (\boldsymbol{q}_D \cdot \nabla) h = \sigma (h \cdot \nabla) \boldsymbol{q}_D + \sigma \frac{Pr_1}{Pr_2} \nabla^2 h, \tag{12}$$

$$\nabla.h = 0, \tag{13}$$

where the dimensionless parameters are given by:

$$T' = \frac{T - T_1}{T_0 - T_1}, \quad p' = \frac{p k_1}{\mu \kappa_m}, \quad \varphi' = \frac{\varphi - \varphi_0}{\varphi_1 - \varphi_0},$$

$$\boldsymbol{q}' = \boldsymbol{q}\frac{d}{\kappa_m}, \quad t' = \frac{t\kappa_m}{\sigma d^2}, \quad (x', y', z') = \frac{(x, y, z)}{d},$$

and $P_r = \frac{\mu}{\rho_f \kappa_m}$; Prandtl number, $D_a = \frac{k_1}{d^2}$; Darcy's number, $V_a = \frac{\epsilon P_r}{D_a}$; Vadasz number, $R_a = \frac{\rho_f g \beta d k (T_0 - T_1)}{\mu_f \kappa_m}$; Rayleigh number, $R_n = \frac{(\rho_p - \rho_f)(\varphi_1 - \varphi_0) g k_1 d}{\mu \kappa_m}$; nanoparticle's Rayleigh number, $L_e = \frac{\kappa_m}{D_B}$; Lewis number, $R_m = \frac{(\rho_p \varphi_0 + \rho_f (1 - \varphi_0)) g k_1 d}{\mu \kappa_m}$; density Rayleigh number, $N_A = \frac{D_T (T_0 - T_1)}{D_B T_1 (\epsilon_1 - \epsilon_0}$; modified diffusivity ratio and $N_B = \frac{\epsilon (\rho c)_p (\varphi_1 - \varphi_0)}{(\rho c)_f}$; modified particle density increment.

The boundary conditions after dimensionless (Chandrasekhar [3] and Nield *et al.* [4, 39]) are

$$\left.\begin{array}{llll} w=0, & \varphi=0 & T=1, & at \quad z=0 \\ w=0, & \varphi=1 & T=0, & at \quad z=1 \end{array}\right\}. \tag{14}$$

2.2. Steady state solutions

The basic state solutions are given by (Buongiorno [2], Sheu [8], Nield and Kuznetsov [12] and Sharma *et al.* [14–16, 22, 29–31])

$$\left.\begin{array}{l} \boldsymbol{q}_D=0 \quad h=(0,0,1) \quad , \\ T=T_b(z), \quad \varphi=\varphi_b(z), \quad p=p_b(z) \end{array}\right\}. \tag{15}$$

Applying equation (15) in equations (9) - (11) reduce to:

$$0=-\frac{d}{dz}p_b(z)-R_m\hat{e}_z+R_aT_b(z)\hat{e}_z-R_n\varphi_b(z)\hat{e}_z+Q\frac{Pr_1}{Pr_2}\left(\frac{\partial h}{\partial z}\right)\hat{k}, \tag{16}$$

$$\frac{d^2}{dz^2}\varphi_b(z)+N_A\frac{d^2}{dz^2}T_b(z)=0, \tag{17}$$

$$\frac{d^2}{dz^2}T_b(z)+\frac{N_B}{L_n}\frac{d}{dz}\varphi_b(z)\frac{d}{dz}T_b(z)+\frac{N_AN_B}{L_n}\left(\frac{d}{dz}T_b(z)\right)^2=0. \tag{18}$$

Using boundary conditions (14) in equation (18), we have

$$\varphi_b(z)=-N_AT_b+(1-z)(1+N_A). \tag{19}$$

Substituting equation (19) in equation (18), we get

$$\frac{d^2}{dz^2}T_b+\frac{(1-N_A)N_B}{L_e}\frac{d}{dz}T_b+\frac{N_AN_B}{L_e}\left(\frac{d}{dz}T_b\right)^2=0,$$

after eliminating the higher order term, we have

$$\frac{d^2}{dz^2}(T_b)+\frac{(1-N_A)N_B}{L_n}\frac{d}{dz}(T_b)=0. \tag{20}$$

Using boundary conditions (14) in equation (16), we get

$$T_b=\frac{e^{-\frac{-N_B(1-N_A)}{L_e}z}\left[1-e^{-\frac{N_B(1-N_A)}{L_e}(1-z)}\right]}{1-e^{-\frac{N_B(1-N_A)}{L_e}}}. \tag{21}$$

Applying Buongiorno [2] hypothesis, equations (19) and (21) reduce to

$$\left.\begin{array}{l} T_b=1-z, \\ \varphi_b=z \end{array}\right\}. \tag{22}$$

Equation (22) is similar to the results of Nield and Kuznetsov [4], Tzou [5, 6], Nield and Kuznetsov [7], Sheu [8], Kuznetsov [12], Sharma *et al.* [29, 30], Nield and Kuznetsov [39] and Yadav *et al.* [40].

2.3. Perturbation solutions

In order to evaluate the stability of the system, we superimpose small perturbation to the basic state equation (15) as

$$\left.\begin{array}{llll} \boldsymbol{q}_D=0+\boldsymbol{q}_D^*, & p=p_b+p^* \\ \varphi=\varphi_b+\varphi^*, & T=T_b+T^*, & h=(0,0,1)+h^* \end{array}\right\}. \tag{23}$$

Using equation (23) in equations (8) - (13), after these pertubations we get linearizing equations as follow

$$\nabla\cdot\boldsymbol{q}_D^*=0, \tag{24}$$

$$\left(\frac{1}{V_a}\frac{\partial}{\partial t}+\frac{1}{1+\lambda_3}\right)\boldsymbol{q}_D^*=-\nabla p^*+R_aT^*\hat{e}_z-R_n\varphi^*\hat{e}_z+Q\frac{Pr_1}{Pr_2}\hat{e}_z\frac{\partial h^*}{\partial z}, \tag{25}$$

$$\frac{1}{\sigma}\frac{\partial\varphi^*}{\partial t}+\frac{\boldsymbol{q}_D^*}{\varepsilon}=\frac{1}{L_e}\nabla^2\varphi^*+\frac{N_A}{L_e}\nabla^2T^*, \tag{26}$$

$$\frac{\partial T^*}{\partial t}-\boldsymbol{q}_D^*=\nabla^2T^*-\frac{N_B}{L_e}(\nabla T^*-\nabla\varphi^*)-\frac{2N_AN_B}{L_e}\nabla T^*, \tag{27}$$

$$\frac{\partial h^*}{\partial t}=\sigma(h.\nabla)\boldsymbol{q}_D^*+\sigma\frac{Pr_1}{Pr_2}\nabla^2h^*, \tag{28}$$

$$\nabla.h^*=0, \tag{29}$$

and the boundary conditions reduce to

$$\left.\begin{array}{llll} w^*=0 & \varphi^*=0 & T^*=0 & at \quad z=0 \\ w^*=0 & \varphi^*=0 & T^*=0 & at \quad z=1 \end{array}\right\}. \tag{30}$$

Operating Eq. (25) with $\hat{e}_z.curl.curl.q_D^*$, we get

$$\left(\frac{1}{V_a}\frac{\partial}{\partial t}+\frac{1}{1+\lambda_3}\right)\nabla^2w^*-R_a\nabla_H^2T^*+R_n\nabla_H^2\varphi^*+Q\frac{\partial^2w^*}{\partial z^2}=0. \tag{31}$$

3. Normal mode and stability analysis

Using normal mode analysis approach for the analysis of perturbations in the system (following Chandrasekhar [3] and and Sharma *et al.* [14–16, 22, 29–31]):

$$[w^*,T^*,\varphi^*]=[W(z),\Theta(z),\Phi(z)]\,e^{(ilx+imy+\omega t)}. \tag{32}$$

Using equation (31) in equations (30), (25) and (26), we get

$$\left[\left(\frac{\omega}{v_a}+\frac{1}{1+\lambda_3}\right)\left(D^2-a^2\right)+QD^2\right]W+a^2R_a\Theta-a^2R_n\Phi=0, \tag{33}$$

$$\frac{1}{\varepsilon}W-\frac{N_A\left(D^2-a^2\right)}{L_e}\Theta-\left(\frac{\left(D^2-a^2\right)}{L_e}-\frac{\omega}{\sigma}\right)\Phi=0, \tag{34}$$

$$W+\left[(D^2-a^2)+\frac{N_B}{L_e}D-2\frac{N_AN_B}{L_e}D-\omega\right]\Theta-\frac{N_B}{L_e}D\Phi=0. \tag{35}$$

Here, $l^2+m^2=a^2$, $\frac{d}{dz}=D$ and a represents dimensionless resultant wave number. Eqs. (33)-(35) with (32) form a characteristic value problem for R_a.

3.1. Free-free boundaries

In this case, the boundary conditions become after the implementation of normal mode as [3]:

$$\left.\begin{array}{llllll} W=0, & D^2W=0, & \Theta=0, & \Phi=0 & at & z=0 \\ W=0, & D^2W=0, & \Theta=0, & \Phi=0 & at & z=1 \end{array}\right\}. \quad (36)$$

3.1.1. Analysis of linear stability and dispersion relation for free-free boundaries

Considering the trial functions for W, Θ and Φ as given below which satisfied equation (36) are

$$W = W_0\ sin\ (\pi z), \quad \Theta = \Theta_0\ sin\ (\pi z), \quad \Phi = \Phi_0\ sin\ (\pi z). \quad (37)$$

Putting equation (37) into equations (33) to (35), and each equation is integrating within the limits 0 to 1 and further by implementation of Galerkin first approximation method then we have the follwing matrix system:

$$\begin{bmatrix} \left(\frac{1}{1+\lambda_3}+\frac{\omega}{V_a}\right)\left(a^2+\pi^2\right)+Q\pi^2 & -a^2R_a & a^2R_n \\ 1 & -\left(a^2+\pi^2\right)-\omega & 0 \\ \frac{1}{\epsilon} & \frac{N_A\left(a^2+\pi^2\right)}{L_e} & \frac{a^2+\pi^2}{L_e}+\frac{\omega}{\sigma} \end{bmatrix} \begin{bmatrix} W_0 \\ \Theta_0 \\ \Phi_0 \end{bmatrix} = \begin{bmatrix} 0 \\ 0 \\ 0 \end{bmatrix}. \quad (38)$$

The non-trivial solution of equation (38) is

$$\begin{vmatrix} \left(\frac{1}{1+\lambda_3}+\frac{\omega}{V_a}\right)\left(a^2+\pi^2\right)+Q\pi^2 & -a^2R_a & a^2R_n \\ 1 & -\left(a^2+\pi^2\right)-\omega & 0 \\ \frac{1}{\epsilon} & \frac{N_A\left(a^2+\pi^2\right)}{L_e} & \frac{a^2+\pi^2}{L_e}+\frac{\omega}{\sigma} \end{vmatrix} = 0. \quad (39)$$

Thus,

$$R_a = \frac{\left(\frac{1}{1+\lambda_3}+\frac{\omega}{V_a}\right)\left(\pi^2+a^2\right)\left(\pi^2+a^2+\omega\right)+Q\pi^2\left(a^2+\pi^2+\omega\right)}{a^2} - \frac{\epsilon N_A\left(\pi^2+a^2\right)+L_e\left(\pi^2+a^2+\omega\right)}{\left(\pi^2+a^2\right)\sigma+\omega L_e}\frac{\sigma}{\epsilon}R_n. \quad (40)$$

Eq. (40) represents the dispersion relation under the effects of λ_3, L_e, R_n, N_A, Q and ϵ.

3.1.2. Non oscillatory convection for free-free boundaries

Putting $\omega = 0$ in equation (40) for steady state and we obtain

$$R_{a_s} = \frac{1}{1+\lambda_3}\frac{\left(a^2+\pi^2\right)^2}{a^2}+Q\frac{\pi^2\left(\pi^2+a^2\right)}{a^2}-\left(N_A+\frac{L_e}{\epsilon}\right)R_n. \quad (41)$$

The critical wave number is obtained by differentiating R_a with respect to a^2 thus the critical wave number must satisfied, i.e.,

$$\left(\frac{\partial R_a}{\partial a^2}\right)_{a=a_c} = 0.$$

Eq. (41) gives

$$a_c = \pi\left[1+Q\left(1+\lambda_3\right)\right]^{1/4}. \quad (42)$$

In the absence of magnetic field Eq. (42) reduces as follow

$$a_c = \pi. \quad (43)$$

Eq. (43) agrees well with the result obtained by Nield *et al.* [12].

3.2. Rigid-rigid boundaries

In this case, the boundary conditions become after the implementation of normal mode as [3]:

$$\left.\begin{array}{llllll} w=0, & \Theta=0, & \Phi=0, & DW=0 & at & z=0 \\ w=0, & \Theta=0, & \Phi=0, & DW=0 & at & z=1 \end{array}\right\}. \quad (44)$$

3.2.1. Analysis of linear stability for rigid-rigid boundaries

Considering W, Θ and Φ are of the form [12]:

$$W = W_0\left(1-z\right)^2 z^2, \quad \Theta = \Theta_0 z\left(1-z\right), \quad \Phi = \Phi_0 z\left(1-z\right), \quad (45)$$

Applying Eq. (45) in Eqs. (33) to (35), each equation integrate within the limits from 0 to 1 and further by implementation of Galerkin first approximation method then we have the following matrix system:

$$\begin{bmatrix} \left(\frac{1}{1+\lambda_3}+\frac{\omega}{V_a}\right)\left(24+2a^2\right)+24Q & -9a^2R_a & 9a^2R_n \\ 3 & -\left(\left(10+a^2\right)+14\omega\right) & 0 \\ \frac{3}{\epsilon} & 14\frac{N_A\left(10+a^2\right)}{L_e} & 14\frac{10+a^2}{L_e}+\frac{14\omega}{\sigma} \end{bmatrix} \begin{bmatrix} W_0 \\ \Theta_0 \\ \Phi_0 \end{bmatrix} = \begin{bmatrix} 0 \\ 0 \\ 0 \end{bmatrix}, \quad (46)$$

the non-trivial solution of equation (46) is

$$\begin{vmatrix} \left(\frac{1}{1+\lambda_3}+\frac{\omega}{V_a}\right)\left(24+a^2\right)+24Q & -9a^2R_a & 9a^2R_n \\ 3 & -\left(14\left(10+a^2\right)+14\omega\right) & 0 \\ \frac{3}{\epsilon} & 14\frac{N_A\left(10+a^2\right)}{L_e} & 14\frac{10+a^2}{L_e}+\frac{14\omega}{\sigma} \end{vmatrix} = 0, \quad (47)$$

which implies that

$$R_a = \frac{28\left[\left(\frac{\omega}{V_a}+\frac{1}{1+\lambda_3}\right)\left(12+a^2\right)+12Q\right]\left(10+a^2+\omega\right)}{27a^2} - \frac{\left[\frac{\left(10+a^2\right)+\omega}{\epsilon}+\frac{N_A\left(10+a^2\right)}{L_e}\right]R_n}{\left[\frac{\left(10+a^2\right)}{L_e}+\frac{\omega}{\sigma}\right]}. \quad (48)$$

3.2.2. Non-oscillatory convection for rigid-rigid boundaries

Putting $\omega = 0$ in equation (48), we obtain

$$R_a + \left(\frac{L_e}{\epsilon}+N_A\right)R_n = \frac{28}{27a^2}\left[\left(12+a^2\right)\left(\frac{1}{1+\lambda_3}\right)+12Q\right]\left(10+a^2\right). \quad (49)$$

The critical wave number is obtained by minimizing R_a with respect to a^2 thus the critical wave number must satisfied, *i.e.*

$$\left(\frac{\partial R_a}{\partial a^2}\right)_{a=a_c} = 0,$$

Therefore, from equation (49), we have

$$a_c = 3.31, \tag{50}$$

which is similar with the result obtained by Nield *et al.* [12].

3.3. Rigid-free boundaries

Following Chandrasekhar [3], the rigid-free boundary conditions after applying normal mode are

$$\left.\begin{array}{llll} w=0, & \Theta=0, & \Phi=0, & DW=0 \quad at \quad z=0 \\ w=0, & \Theta=0, & \Phi=0, & D^2W=0 \quad at \quad z=1 \end{array}\right\}. \tag{51}$$

3.3.1. Analysis of linear stability for rigid-free boundaries

Considering W, Θ and Φ are of the form (Nield *et al.* [12])

$$W = W_0 z^2 (1-z)(3-2z) z^2, \Theta = \Theta_0 z (1-z), \Phi = \Phi_0 z (1-z), \tag{52}$$

Putting Eq. (52) into Eqs. (33)-(35), on integrating within limits from 0 to 1 and further by implementation of Galerkin first approximation method then we have the follwing matrix system:

$$\begin{bmatrix} \left(\frac{1}{1+\lambda_3}+\frac{\omega}{V_a}\right)\left(\frac{12}{35}+\frac{19a^2}{630}\right)+Q\frac{12}{35} & -\frac{13}{420}a^2R_a & \frac{13}{420}{}^2R_n \\ \frac{13}{420} & -\left[\left(\frac{1}{3}+\frac{a^2}{30}\right)+\frac{\omega}{30}\right] & 0 \\ \frac{13}{420\epsilon} & \frac{N_A}{L_e}\left(\frac{1}{3}+\frac{a^2}{30}\right) & \frac{1}{L_e}\left(\frac{1}{3}+\frac{a^2}{30}\right)+\frac{\omega}{30\sigma} \end{bmatrix} \begin{bmatrix} W_0 \\ \Theta_0 \\ \Phi_0 \end{bmatrix} = \begin{bmatrix} 0 \\ 0 \\ 0 \end{bmatrix}, \tag{53}$$

the non-trivial solution of equation (53) is

$$\begin{vmatrix} \left(\frac{1}{1+\lambda_3}+\frac{\omega}{V_a}\right)\left(\frac{12}{35}+\frac{19a^2}{630}\right)+Q\frac{12}{35} & -\frac{13}{420}a^2R_a & \frac{13}{420}{}^2R_n \\ \frac{13}{420} & -\left[\left(\frac{1}{3}+\frac{a^2}{30}\right)+\frac{\omega}{30}\right] & 0 \\ \frac{13}{420\epsilon} & \frac{N_A}{L_e}\left(\frac{1}{3}+\frac{a^2}{30}\right) & \frac{1}{L_e}\left(\frac{1}{3}+\frac{a^2}{30}\right)+\frac{\omega}{30\sigma} \end{vmatrix} = 0, \tag{54}$$

which implies that

$$R_a = \frac{28\left[\left(\frac{\omega}{V_a}+\frac{1}{1+\lambda_3}\right)\left(216+19a^2\right)+216Q\right]\left(10+a^2+\omega\right)}{507a^2} - \frac{\left[\frac{(10+a^2)+\omega}{\epsilon}+\frac{N_A(10+a^2)}{L_e}\right]R_n}{\left[\frac{(10+a^2)}{L_e}+\frac{\omega}{\sigma}\right]}. \tag{55}$$

3.3.2. Non-oscillatory convection for rigid-free boundaries

For this, putting $\omega = 0$ in above equation (55), we get

$$R_a + \left(\frac{L_e}{\epsilon}+N_A\right)R_n = \frac{28}{507a^2}\left[\left(216+19a^2\right)\left(\frac{1}{1+\lambda_3}\right)+216Q\right]\left(10+a^2\right). \tag{56}$$

The critical wave number is obtained by minimizing R_a with respect to a^2 thus the critical wave number must satisfied, *i.e.*

$$\left(\frac{\partial R_a}{\partial a^2}\right)_{a=a_c} = 0.$$

The above equation (56) gives

$$a_c = 3.27. \tag{57}$$

This result is similar with the result obtained by Nield *et al.* [12].

4. Results and discussion

In this paper, we have analysed the effect of magnetic field on the onset of thermal convection in a Jeffery nanofluid layer saturated by a porous medium for free-free, rigid-rigid and rigid-free boundary conditions. The effects of various parameters like; λ_3, L_e, R_n, N_A, Q and ϵ on stationary convection are represented graphically as shown by Figures 2-7 for free-free, rigid-rigid and rigid-free boundary conditions.

Figure 2 represents the graph between R_{a_s} and wave number a for the distinct values of $\lambda_3 = 0.3, 0.5, 0.9$ by fixing the other parameters as $N_A = 10$, $L_e = 1000$, $\epsilon = 0.6$, $R_n = -1$ and $Q = 100$. It is clear from Figure 2 that within the increase in the value of λ_3 *i.e.* Jeffrey parameter, R_{a_s} goes on decreasing and hence as a result of this behaviour Jeffrey parameter shows the destabilising effect on stationary convection. Also, we can see from Figure 2 that in case of rigid-free boundary conditions, the system has more destabilising impact on stationary convection in comparison with free-free and rigid-rigid boundary conditions. Thus, λ_3 *i.e.*, Jeffrey parameter enhances the onset of convection. Figure 3 represents the graph between R_{a_s} and wave number a for distinct values of $Q = 50, 100, 150$ by fixing the other parameters as $N_A = 10$, $L_e = 1000$, $\lambda_3 = 0.5$, $R_n = -1$ and $\epsilon = 0.6$. We observed from the Figure 3 that as the value of Q increases, R_{a_s} goes on increasing and hence Q shows the stabilising effect on stationary convection. Also, we can see from Figure 3 that in case of free-free boundary conditions, Q has more stabilising impact on stationary convection in comparison with rigid-free and rigid-rigid boundary conditions. Thus, Q delays the onset of convection. Figure 4 represents the graph between R_{a_s} and wave number a for distinct values of $R_N = -1, -0.5, -0.1$, by fixing the other parameters as $N_A = 10$, $L_e = 1000$, $\lambda_3 = 0.5$, $\epsilon = 0.6$ and $Q = 100$. We observed from Figure 4 that as R_N increases, R_{a_s} goes on decreasing and hence shows the destabilising effect on stationary convection. Figure 4 also demonstrates that for rigid-free boundary conditions R_N

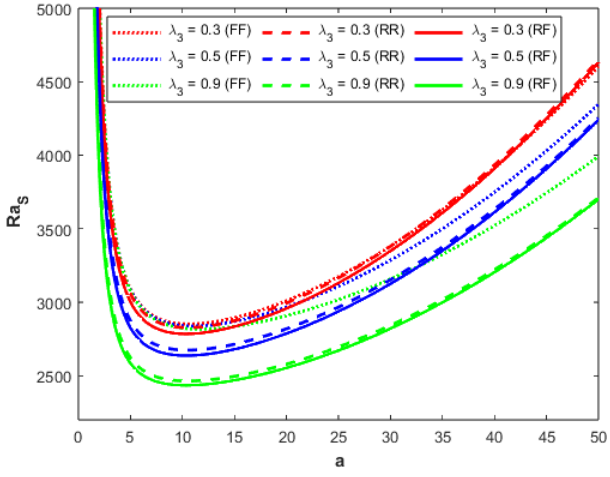

Figure 2. R_{a_s} versus a for the distinct values of λ_3.

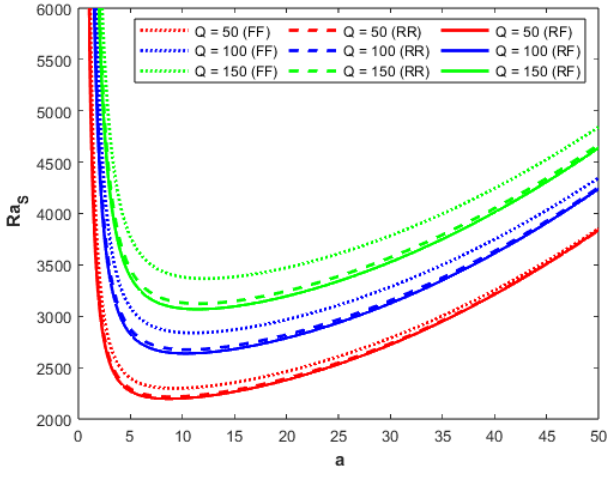

Figure 3. R_{a_s} versus a for the distinct values of Q.

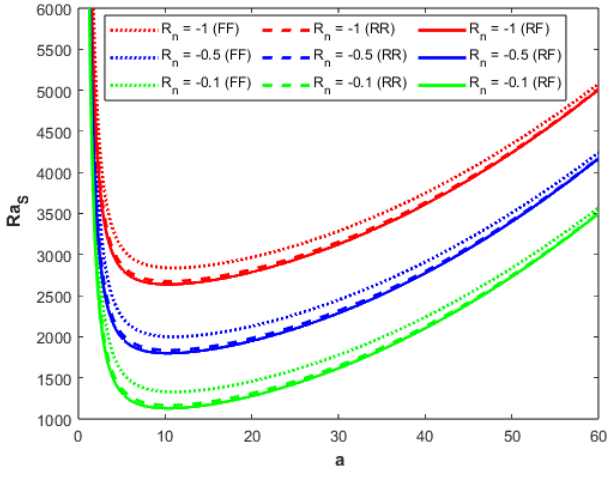

Figure 4. R_{a_s} versus a for the distinct values of R_n.

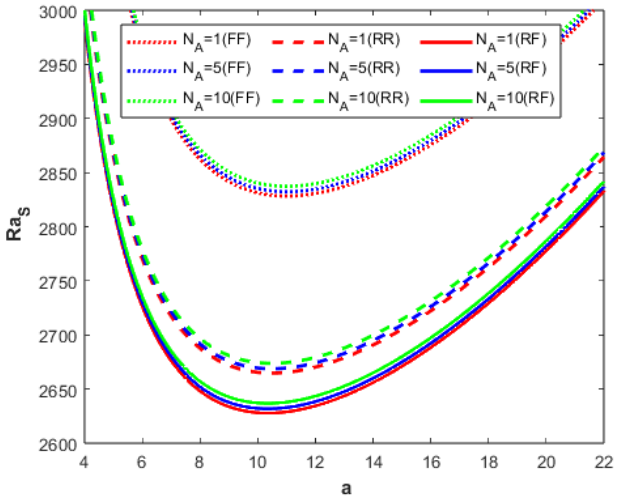

Figure 5. R_{a_s} versus a for the distinct values of N_A.

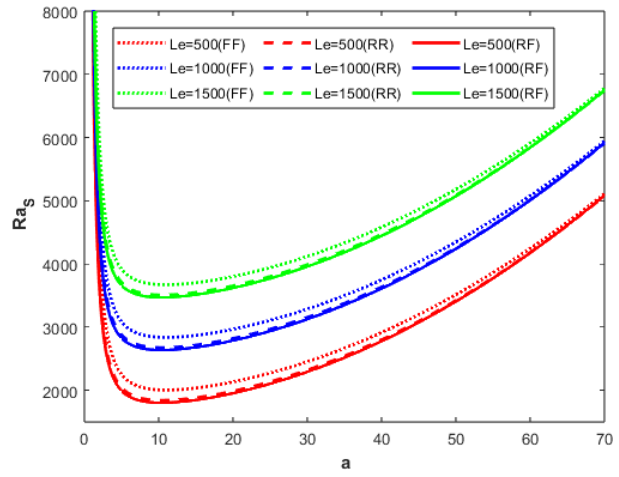

Figure 6. R_{a_s} versus a for the distinct values of L_e.

has more destabilising impact on stationary convection as compared to free-free and rigid-rigid boundary conditions. Thus, R_N accelerates the onset of convection.

Figure 5 represents the graph of R_{a_s} against the wave number a for distinct values of $N_A = 1, 5, 10$, while fixing the other parameters as $\epsilon = 0.6$, $L_e = 1000$, $\lambda_3 = 0.5$, $R_n = -1$, and $Q = 100$. From Figure 5, it is observed that as the values of N_A increase, R_{a_s} also increases, demonstrating a stabilizing effect on stationary convection. Additionally, it is evident from Figure 5 that free-free boundary conditions have a more stabilizing impact on stationary convection compared to other boundary conditions. Therefore, N_A delays the system.

Figure 6 represents the graph between R_{a_s} and wave number a for distinct values of $L_e = 500, 1000, 1500$ by fixing the other parameters as $N_A = 10$, $\epsilon = 0.6$, $\lambda_3 = 0.5$, $R_n = -1$, and $Q = 100$. We observe from Figure 6 that as we increase L_e, R_{a_s} also increases, resulting in L_e showing a stabilizing effect on stationary convection. This investigation also demonstrates,

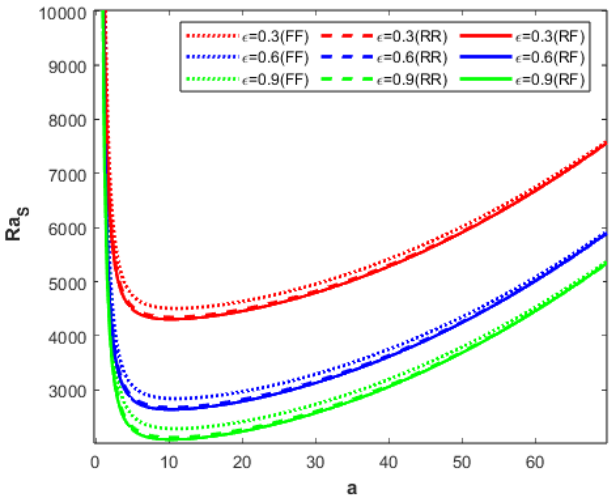

Figure 7. R_{a_s} versus a for the distinct values of ϵ.

after analyzing Figure 6, that for free-free boundary conditions, L_e has a more stabilizing impact on stationary convection compared to other boundary conditions. Thus, L_e delays the onset of convection.

Figure 7 represents the graph between R_{a_s} and the wave number a for distinct values of $\epsilon = 0.3, 0.6, 0.9$, while fixing the other parameters as $N_A = 10$, $L_e = 1000$, $\lambda_3 = 0.5$, $R_n = -1$, and $Q = 100$. We observed from Figure 7 that with the increase in the values of ϵ, R_{a_s} decreases, thereby demonstrating the destabilizing effect of ϵ on stationary convection. Additionally, it is evident from Figure 7 that for rigid-free boundary conditions, ϵ has a more destabilizing impact on stationary convection compared to rigid-rigid and free-free boundary conditions. Thus, ϵ also enhances the onset of convection.

5. Conclusion

In this research paper, we have analyzed the thermal instability of the Jeffery nanofluid layer in the presence of a magnetic field for all boundary conditions. We have investigated the effects of various parameters such as λ_3, L_e, R_n, N_A, Q, and ϵ on stationary convection both analytically and graphically for free-free, rigid-rigid, and rigid-free boundary conditions. This entire investigation is carried out with the help of Galerkin's first approximation and normal mode analysis.

From our investigation, we have drawn the following conclusions:

1. The Chandershekar number Q has a stabilizing impact on the onset of convection, producing a behavior that delays the onset of convection.
2. Parameters like the Jeffery parameter (λ_3), the nanoparticle's Rayleigh number R_n, and the medium porosity ϵ have destabilizing effects on stationary convection, accelerating its onset.
3. Parameters such as the Lewis number L_e and the modified diffusivity ratio N_A introduce stabilizing effects on the system, delaying the onset of convection.
4. It is discovered that the three parameters, namely λ_3, R_n, and ϵ, exhibit a greater destabilizing influence on rigid-free boundaries, accelerating the onset of convection more quickly in such conditions.
5. Conversely, the Lewis number, Chandrasekhar number, and modified diffusivity ratio show a greater stabilizing influence in free-free boundaries compared to rigid-free and rigid-rigid boundaries. This indicates a delay in the onset of convection due to these parameters. Consequently, in the case of free-free boundary conditions, the magnetic field parameter causes a greater delay in the onset of convection compared to rigid-rigid and rigid-free boundary conditions.
6. This study mainly focuses on the impacts of the magnetic field and Jeffrey nanofluid on the onset of convection. The magnetic field results in the occurrence of the Chandrasekhar number, which exhibits more stabilizing behavior in free-free boundary conditions. Meanwhile, the implementation of the Jeffrey nanofluid accelerates the onset of convection due to its destabilizing effect on the system.

Acknowledgment

The author(s) gratefully thankful to the Chairman of Department of Mathematics & Statistics, Himachal Pradesh University, Shimla for providing congenial atmosphere for research.

References

[1] S.U. Choi & J. A. Eastman, *Enhancing thermal conductivity of fluids with nanoparticles*, Technical report, Argonne National Lab.(ANL), Argonne, IL (United States), 1995. https://www.osti.gov/servlets/purl/196525.

[2] J. Buongiorno, "Convective transport in nanofluids", Transactions of the ASME **128** (2006) 240. https://doi.org/10.1115/1.2150834.

[3] S. Chandrasekhar, "*Hydrodynamic and hydromagnetic stability*", Dover Publications, Inc., New York, U.S.A., 2013, pp. 1-704. https://www.google.co.in/books/edition/Hydrodynamic_and_Hydromagnetic_Stability/Mg3CAgAAQBAJ?hl=en&gbpv=1&dq=Hydrodynamic+and+Hydromagnetic+Stability&pg=PP1&printsec=frontcover.

[4] D. Nield & A. V. Kuznetsov, "Thermal instability in a porous medium layer saturated by a nanofluid", International Journal of Heat and Mass Transfer **52** (2009) 5796. https://doi.org/10.1016/j.ijheatmasstransfer.2009.07.023.

[5] D. Tzou, "Instability of nanofluids in natural convection", Journal of Heat Transfer **130** (2008) 072401. https://doi.org/10.1115/1.2908427.

[6] D. Y. Tzou, "Thermal instability of nanofluids in natural convection", International Journal of Heat and Mass Transfer **51** (2008) 2967. https://doi.org/10.1016/j.ijheatmasstransfer.2007.09.014.

[7] D. A. Nield & A. Bejan, "*Convection in Porous Media*", Springer Cham, Switzerland, 2006, pp. 1-988. https://doi.org/10.1007/978-3-319-49562-0

[8] L. J. Sheu, "Thermal instability in a porous medium layer saturated with a viscoelastic nanofluid", Transport in Porous Media **88** (2011) 461. https://doi.org/10.1007/s11242-011-9749-2.

[9] G. C. Rana & P. K. Gautam, "On the onset of thermal instability of a porous medium layer saturating a Jeffrey nanofluid", Engineering Transactions **70** (2022) 123. https://doi.org/10.24423/EngTrans.1387.20220609.

[10] P. L. Sharma, Deepak & A. Kumar, "Effects of rotation and magnetic field on thermosolutal convection in elastico- viscous Walters' (Model B') nanofluid with porous medium", Stochastic Modeling & Applications

26 (2022) 21. https://www.researchgate.net/publication/371416130_EFFECTS_OF_ROTATION_AND_MAGNETIC_FIELD_ON_THERMOSOLUTAL_CONVECTION_IN_ELASTICO-_VISCOUS_WALTERS_MODEL_B_NANOFLUID_WITH_POROUS_MEDIUM.

[11] P. L. Sharma, M. Kapalta, A. Kumar, D. Bains & P. Thakur, "Electrohydro dynamics convection in dielectric rotating Oldroydian nanofluid in porous medium", Journal of the Nigerian Society of Physical Sciences **5** (2023) 1231. https://doi.org/10.46481/jnsps.2023.1231

[12] A. Kuznetsov & D. Nield, "Thermal instability in a porous medium layer saturated by a nanofluid: Brinkman model", Transport in Porous Media **81** (2010) 409. https://doi.org/10.1007/s11242-009-9413-2.

[13] P. K. Gautam, G. C. Rana & H. Saxena, "Stationary convection in the electrohydrodynamic thermal instability of Jeffrey nanofluid layer saturating a porous medium: free-free, rigid-free, and rigid-rigid boundary conditions", Journal of Porous Media **23** (2020) 1043. https://doi.org/10.1615/JPorMedia.2020035061.

[14] P. L. Sharma, D. Bains & P. Thakur, "Thermal instability of rotating Jeffrey nanofluids in porous media with variable gravity", Journal of the Nigerian Society of Physical Sciences **5** (2023) 1366. https://doi.org/10.46481/jnsps.2023.1366

[15] P. L. Sharma, D. Bains, A. Kumar & P. Thakur, "Effect of rotation on thermosolutal convection in Jeffrey nanofluid with porous medium", Structural Integrity and Life **23** (2023) 299. http://divk.inovacionicentar.rs/ivk/ivk23/299-IVK3-2023-PLS-DB-AK-PT.pdf.

[16] P. L. Sharma, A. Kumar, D. Bains, P. Lata & P. Thakur, "Thermal convective instability in a Jeffrey nanofluid saturating a porous medium: rigid-rigid and rigid-free boundary conditions", Structural Integrity and Life **23** (2023) 351. http://divk.inovacionicentar.rs/ivk/ivk23/351-IVK3-2023-PLS-AK-DB-PL-GCR.pdf.

[17] G. C. Rana, "Effects of rotation on Jeffrey nanofluid flow saturated by a porous medium", Journal of Applied Mathematics and Computational Mechanics **20** (2021) 17. https://doi.org/10.17512/jamcm.2021.3.02.

[18] S. U. Khan, Usman, A. Raza, A. Kanwal & K. Javid, "Mixed convection radiated flow of Jeffery-type hybrid nanofluid due to inclined oscillating surface with slip effects: a comparative fractional model", Waves in Random and Complex Media (2022) 1. https://doi.org/10.1080/17455030.2022.2122628.

[19] A. K. Pati, A. Misra, S. K. Mishra, S. Mishra, R. Sahu & S. Panda, "Computational modelling of heat and mass transfer optimization in copper water nanofluid flow with nanoparticle ionization", JP Journal of Heat and Mass Transfer **31** (2023) 1. https://doi.org/10.17654/0973576323001.

[20] A. K. Pati, A. Misra & S. K. Mishra, "Effect of electrification of nanoparticles on heat and mass transfer in boundary layer flow of a copper water nanofluid over a stretching cylinder with viscous dissipation", JP Journal of Heat and Mass Transfer **17** (2019) 97. http://dx.doi.org/10.17654/HM017010097.

[21] M. B. Ashraf, A. Tanveer & S. Ulhaq, "Effects of Cattaneo-Christov heat flux on MHD Jeffery nano fluid flow past a stretching cylinder", Journal of Magnetism and Magnetic Materials **565** (2019) 170154. https://doi.org/10.1016/j.jmmm.2022.170154.

[22] P. L. Sharma, D. Bains & G. C. Rana, "Effect of variable gravity on thermal convection in Jeffrey nanofluid: Darcy-Brinkman Model", Numerical Heat Transfer, Part B: Fundamentals (2023) 1. https://doi.org/10.1080/10407790.2023.2256970.

[23] D. Bains, P. L. Sharma & G. C. Rana, "Effect of variable gravity on thermal convection in rotating Jeffrey nanofluid: Darcy-Brinkman model", Special Topics & Reviews in Porous Media: An International Journal **15** (2024) 25. https://doi.org/10.1615/SpecialTopicsRevPorousMedia.2023049875.

[24] A. Garg, Y. D. Sharma & S. K. Jain, "Stability analysis of thermobioconvection flow of Jeffrey fluid containing gravitactic microorganism into an anisotropic porous medium", Forces in Mechanics **10** (2023) 100152. https://doi.org/10.1016/j.finmec.2022.100152.

[25] A. Garg, Y. D. Sharma & S. K. Jain, "Instability investigation of Thermobioconvection of oxytactic microorganism in Jeffrey nanoliquid with effects of internal heat source", Journal of Porous Media **26** (2023) 13. https://doi.org/10.1615/JPorMedia.2023046406.

[26] A. Garg, Y. D. Sharma & S. K. Jain, "Onset of triply diffusive thermo-bio-convection in the presence of gyrotactic microorganisms and internal heating into an anisotropic porous medium: oscillatory convection", Chinese Journal of Physics **84** (2023) 173. https://doi.org/10.1016/j.cjph.2023.05.014.

[27] A. Garg, Y. D. Sharma, S. K. Jain & S. Maheshwari, "Numerical study of the influence of magnetic field and throughflow on the onset of thermo-bio-convection in a Forchheimer-extended Darcy-Brinkman porous nanofluid layer containing gyrotactic microorganisms", Journal of Porous Media (2024) 77. https://doi.org/10.1615/JPorMedia.2024049980.

[28] A. Garg, Y. D. Sharma & S. K. Jain, "Impact of an anisotropic porous media on thermobioconvection instability in the presence of gyrotacticmicroorganisms and heating from below", Special Topics & Reviews in Porous Media: An International Journal **15** (2024) 1. https://doi.org/10.1615/SpecialTopicsRevPorousMedia.2023048137.

[29] D. Bains & P. L. Sharma, "Thermal instability of hydro-magnetic Jeffrey nanofluids in porous media with variable gravity for: free-free, rigid-rigid and rigid-free boundaries", Special Topics & Reviews in Porous Media: An International Journal **15** (2023) 51. https://doi.org/10.1615/SpecialTopicsRevPorousMedia.2023048444.

[30] P. L. Sharma, A. Kumar, D. Bains & G. C. Rana, "Effect of magnetic field on thermosolutal convection in Jeffrey nanofluid with porous medium", Special Topics & Reviews in Porous Media: An International Journal **14** (2023) 17. https://doi.org/10.1615/SpecialTopicsRevPorousMedia.2023046929.

[31] P. L. Sharma, A. Kumar, M. Kapalta & D. Bains, "Effect of magnetic field on thermosolutal convection in a rotating non-Newtonian nanofluid with porous medium", International Journal of Applied Mathematics & Statistical Sciences **12** (2023) 19. https://www.researchgate.net/publication/374616576_EFFECT_OF_MAGNETIC_FIELD_ON_THERMOSOLUTAL_CONVECTION_IN_A_ROTATING_NON-NEWTONIAN_NANOFLUID_WITH_POROUS_MEDIUM.

[32] D. Yadav, "Influence of anisotropy on the Jeffrey fluid convection in a horizontal rotary porous layer", Heat Transfer **50** (2021) 4595. https://doi.org/10.1002/htj.22090.

[33] D. Yadav, "Effect of electric field on the onset of Jeffery fluid convection in a heat-generating porous medium layer", Pramana **96** (2022) 19. https://doi.org/10.1007/s12043-021-02242-6.

[34] D. Yadav, "Thermal non-equilibrium effects on the instability mechanism in a non-Newtonian Jeffrey fluid saturated porous layer", Journal of Porous Media **25** (2022) 1. https://doi.org/10.1615/JPorMedia.2021038392.

[35] D. Yadav, "Numerical treatment on the convective instability in a Jeffrey fluid soaked permeable layer with through-flow", Mathematical Modeling for Intelligent Systems **1** (2022) 11. https://www.taylorfrancis.com/chapters/edit/10.1201/9781003291916-10/numerical-treatment-convective-instability-jeffrey-fluid-soaked-permeable-layer-flow-dhananjay-yadav-mukesh-kumar-awasthi-mahabaleshwar-krishnendu-bhattacharyya.

[36] D. Yadav, A. A. Mohamad & M. K. Awasthi, "The Horton–Rogers–Lapwood problem in a Jeffrey fluid influenced by a vertical magnetic field. Proceedings of the Institution of Mechanical Engineers", Part E: Journal of Process Mechanical Engineering **235** (2021) 2119. https://doi.org/10.1177/09544089211031108.

[37] D. Yadav, S. Al-Balushi, M. K. Awasthi, T. Al-Hadi, R. Al-Abri, J. Al-Wahaibi, F. Al-Nasseri, S. Al-Siyabi, R. Ragoju & K. Bhattacharyya, "Convective flow of ethylene glycol-silver Jeffery nanofluid in a Hele-Shaw cell with an influence of external magnetic field", Asia-Pacific Journal of Chemical Engineering **18** (2023) 2884. https://doi.org/10.1002/apj.2884.

[38] U. Gupta, J. Ahuja & R. K. Wanchoo, "Magneto convection in a nanofluid layer.", International Journal of Heat and Mass Transfer **64** (2013) 1163. https://doi.org/10.1016/j.ijheatmasstransfer.2013.05.035.

[39] D. Nield & A. V. Kuznetsov, "The onset of convection in a horizontal nanofluid layer of finite depth", European Journal of Mechanics-B/Fluids **29** (2010) 217. https://doi.org/10.1016/j.euromechflu.2010.02.003.

[40] D. Yadav, R. Bhargava & G. S. Agrawal, "Boundary and internal heat source effects on the onset of Darcy–Brinkman convection in a porous layer saturated by nanofluid", International Journal of Thermal Sciences **60** (2012) 244. https://doi.org/10.1016/j.ijthermalsci.2012.05.011.